



ISSN: 0067-2904

## Synthesis and Characterization of $\text{Cu}_2\text{FeSnSe}_4$ Nanofilms

Omar Abdulsada Ali\*, Sarmed S.M. Al-Awadi

Department of Physics, College of Science, University of Baghdad, Baghdad, Iraq

Received: 10/2/2020

Accepted: 29/9/2020

### Abstract

Well dispersed  $\text{Cu}_2\text{FeSnSe}_4$  (CFTSe) nanofilms were synthesized by hot-injection method. The structural and morphological measurements were characterized using XRD (X-ray diffraction), Raman spectroscopy, SEM (scanning electron microscopy), and TEM (transmission electron microscopy). Chemical composition and optical properties of as-synthesized CFTSe nanoparticles were characterized using EDS (energy dispersive spectroscopy) and UV-Vis spectrophotometry. The average particle size of the nanoparticles was about 7-10 nm. The UV-Vis absorption spectra showed that the synthesized CFTS nanofilms have a band gap ( $E_g$ ) of about 1.16 eV. Photo-electrochemical characteristics of CFTSe nanoparticles were studied and indicated their potential application in photovoltaic applications.

**Keywords:**  $\text{Cu}_2\text{FeSnSe}_4$ , nanofilms, hot-injection, photo-electrochemistry.

### تحضير وتوصيف أغشية النانوية $\text{Cu}_2\text{FeSnSe}_4$

عمر عبد السادة علي\* ، سرمد صالح مهدي

قسم الفيزياء، كلية العلوم، جامعة بغداد، العراق، بغداد.

### الخلاصة

تم تحضير الأغشية النانوية  $\text{Cu}_2\text{FeSnSe}_4$  (CFTSe) بطريقة الحقن الساخن. تم إجراء قياسات التركيب البلوري والسطحي والكيميائي والخصائص البصرية لجسيمات CFTSe النانوية باستخدام حيود الأشعة السينية (XRD)، وطيف رامان، مطيافية تشتت الطاقة (EDS)، والمجهر الماسح الإلكتروني (SEM) و المجهر الإلكتروني النافذ (TEM) و UV-Vis وكان متوسط أحجام الجسيمات النانوية حوالي 7-10 نانومتر. قدرت فجوة الطاقة للأغشية النانوية CFTS بحوالي 1.16 إلكترون فولت. تمت دراسة الخصائص الكهروكيميائية الضوئية للجسيمات النانوية CFTSe، مما يشير إلى تطبيقها المحتمل في التطبيقات الفوتوفولطانية.

### Introduction

Semiconductor compounds, such as the ternary and multinary ones, received a significant interest in the recent years due to their physical properties and technological applications [1,2].  $\text{I}_2\text{-II-IV-VI}_4$  can be considered as one of the two available groups of fourfold normal derivative ( $\text{A}_2\text{BCD}_4$ ) of the II-VI binaries, in which there are three types of cations instead of cation II. Among these,  $\text{Cu}_2\text{ZnSnS}_4$  (CZTS),  $\text{Cu}_2\text{FeSnS}_4$  (CFTS),  $\text{Cu}_2\text{ZnSnSe}_4$  (CZTSe) and  $\text{Cu}_2\text{FeSnSe}_4$  (CFTSe) received additional interest due to their earth-abundance and identical crystal structures to  $\text{CuInGaSe}_2$  (CIGSe) [3-6]. The conversion efficiency of (CZTS-based) solar cells was reported to approach the value of 12.6% [7].

\*Email: prof.lai2014@gmail.com

Due to its optimum  $E_g$  ( $\sim 1.5$  eV), the quaternary semiconductor CFTSe has been used as an alternative choice with a high absorption coefficient ( $>10^4$  cm $^{-1}$ ). Nevertheless, the photo-electronic properties of CFTSe are still partially unstudied.

A hydrothermal method was formerly used to synthesize CFTSe nano-sheets [8]. Here we report the synthesis of CFTSe nano-crystals by the hot-injection method, which represents a major function in the large-scale fabrication of solar cells based on the synthesis of nanocrystals. This process decreases fabrication costs compared with the conventional physical vapor deposition (PVD) technique [9, 10], which is a contribution to the development of low-cost photoelectronic devices.

In this paper, the growth procedure was examined preliminarily. The structural, morphological, and optical properties of CFTSe nanoparticles were investigated. These nano-crystals can be readily dispersed in solvents which have low toxicity and are good fabricated into CFTSe films by drop-casting. The photo-electrochemical response of the obtained film was also investigated. Our study is a contribution to put forward the photoelectric device applications of CFTSe nanocrystals.

## Experiments

### Materials

$\text{CuCl}_2 \cdot 2\text{H}_2\text{O}$  (Copper II chloride dihydrate),  $\text{FeCl}_2$  (Iron II chloride),  $\text{SnCl}_4 \cdot 5\text{H}_2\text{O}$  (tin IV tetrachloride pentahydrate), selenium powder, DPP (diketopyrrolopyrrole) and OLA (Oleylamine) were purchased from Sigma-Aldrich Chemical Co.

### Synthesis of CFTSe nanoparticles

In a perfect synthesis process, a mix of (0.2 mmol)  $\text{CuCl}_2 \cdot 2\text{H}_2\text{O}$ , (0.1 mmol)  $\text{FeCl}_2$ , (0.1 mmol)  $\text{SnCl}_4 \cdot 5\text{H}_2\text{O}$ , and (10 ml) OLA were dissolved in a 3-neck bottle at Ar atmosphere. The solution was magnetically stirred and heated to 553 K. selenium powder (0.4 mmol) was dispersed in 5 ml DPP to form DPP-Se complex in a glove box. At a reaction temperature of 553 K, 5ml DPP-Se was injected into the three neck bottle and kept for 5 minutes. After reaction, CFTSe nanoparticles were centrifuged using alcohol and toluene. Figure- 1 A and B show the schematic representation and SEM image of CFTSe nanoparticles which were sprayed onto FTO substrates, followed by the deposition of 15 nm CdS layer onto CFTSe thin film via chemical bath deposition (CBD) method. At last, a 5 nm Pt electrode layer was sputtered on CdS thin film surface.

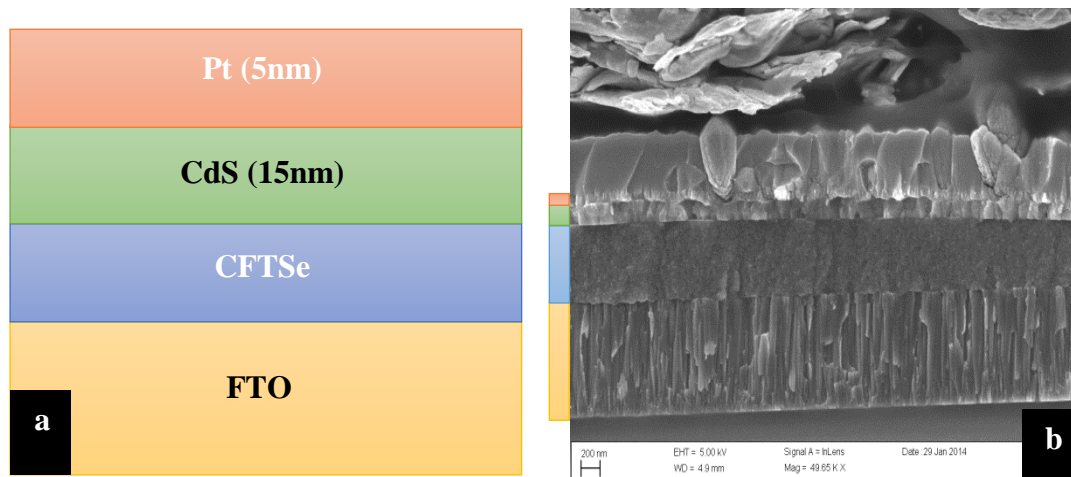


**Figure 1-** (a) Schematic representation and (b) SEM image of FTO/ CFTSe /CdS/Pt.

### Characterization

The microstructures and the crystal of the prepared samples were characterized by XRD using a (Rigaku R-Axis Spider diffractometer) with  $\text{Cu K}\alpha$  ( $\lambda = 1.54$  Å) radiation operated at 40 kV and 40 mA and an image-plate detector. The phase purities of CFTSe nano-particles were examined by Raman spectra (JY-H800UV). UV-vis (Jasco UV-570) spectrophotometer was used to study the optical properties of CFTSe nanoparticles. The morphological properties of CFTSe nanoparticles were characterized using SEM FEI Sirion 200 and JEOL 2010F TEM at 200 kV accelerating voltage. The photocurrent-time response of the CFTSe thin films was measured in 0.5 M of  $\text{Na}_2\text{SO}_4$  (pH=0.5) under 100 mW/cm $^2$  (AM 1.5 G) light source. FTO/ CFTSe and FTO/ CFTSe /CdS/Pt were fabricated as the efficient electrodes.

## Results and discussion

XRD patterns of CFTSe nano-particles are demonstrated in Figure- 2. Obvious diffraction peaks appeared at  $27.17^\circ$ ,  $45.07^\circ$ ,  $53.41^\circ$ ,  $65.65^\circ$ ,  $72.41^\circ$  and  $83.22^\circ$ , which correspond to (112), (204), (116), (400), (316) and (422) of CFTSe tetragonal structures, respectively (PDF No. 52-0998). According to FWHM (full width of half maximum), the values of (112) diffraction peak, their average crystallite sizes were estimated to be about 10 nm, using Scherrer's equation:

$$D = \frac{0.9\lambda}{\beta \cos\theta} \quad (1)$$

where  $D$  is the grain crystallite diameter,  $\theta$  is the peak location, and  $\beta$  is the half-width of the diffraction peak at half height [11, 12].

As known,  $\text{Cu}_2\text{SnSe}_3$  and  $\text{Cu}_2\text{Se}$  have crystal structures which are very close to that of CFTSe. Thus, Raman characterizations were performed to examine the phase purity of CFTSe nanoparticle thin films. Three obvious peaks appeared at  $209$ ,  $267$  and  $378 \text{ cm}^{-1}$  which confirmed the main products of CFTSe. No Raman peaks at  $180$ ,  $236$ ,  $251$  and  $260 \text{ cm}^{-1}$  were found, which indicates that no secondary phases, such as  $\text{Cu}_2\text{SnSe}_3$ ,  $\text{CuSe}$  and  $\text{Cu}_2\text{Se}$ , existed [11, 12].

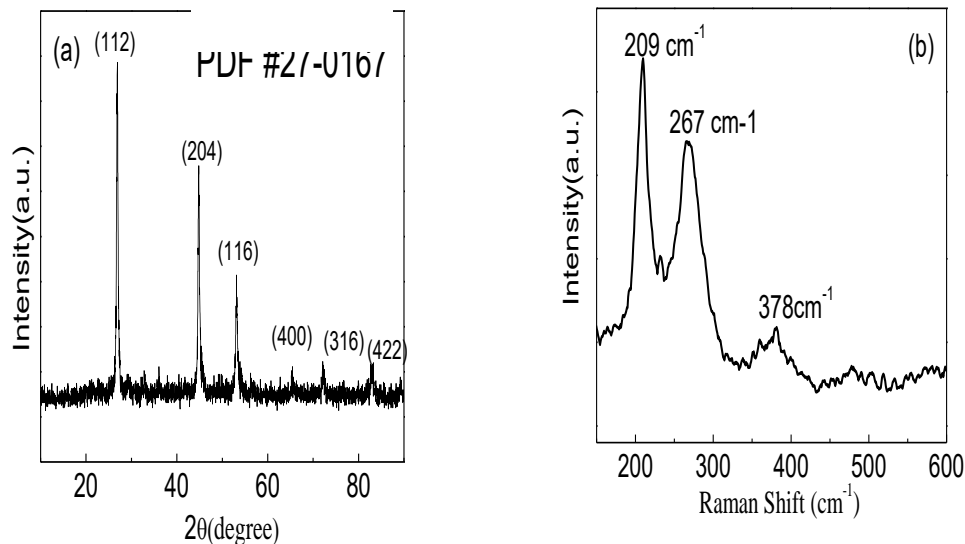


**Figure 2-** (a) XRD and (b) Raman spectra of CFTSe nanofilms.

The synthesized CFTSe nano-particles were dip-coated onto FTO substrates and the surface properties were characterized by SEM. As shown in Figure- 3, the surface of CFTSe thin films was very compact and composed of small nanoparticles. The figure shows that the film surface had relatively homogeneous polycrystalline grain structure. The atomic composition ratio of CFTSe nanoparticles was  $20.1 : 12.2 : 13.4 : 54.3$  as indicated by EDS measurements. The TEM images proved that the nanocrystals are regular in shape and have mono-disperse, i.e. similar in size and shape. TEM characterizations indicated that CFTSe nanoparticles have uniform average sizes, which are about 8-10 nm, which agreed well with those calculated by XRD. HRTEM image shows that the (220) peak of CFTSe sheets is equal to  $2.01 \text{ \AA}$  interplanar spacing. The diffraction spot of (111) plane in the image of the selected area electron diffraction (SAED) indicates the single crystal nature of CFTSe nanoparticles.

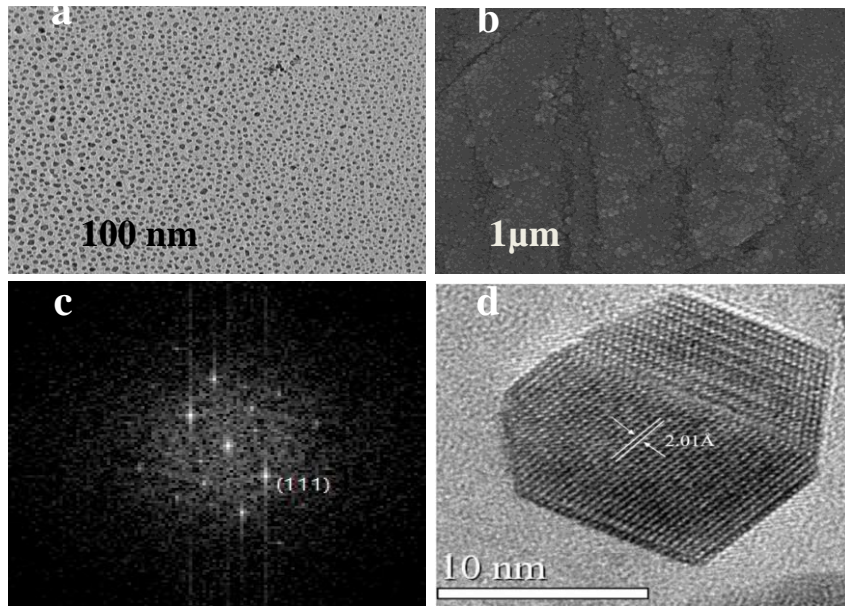


**Figure 3-** (a) TEM, (b) SEM, (c) SAED pattern and (d) HRTEM of CFTSe nanofilms.

CFTSe nanoparticles were dispersed in chloroform and their absorption spectra are presented in Figure- 4. As shown, CFTSe nanofilms have an obvious absorption in the visible light range and their band-gaps were determined to be about 1.16 eV, according to Tauc law which could be used to obtain the band gap energy of CFTSe nanofilms [13, 14], as follows.

$$\alpha (h\nu) = A (h\nu - E_g)^r \quad (2)$$

where A is a constant and inversely proportional to amorphously,  $\alpha$  is the absorption coefficient,  $h$  the Planck constant,  $\nu$  is the frequency, and  $E_g$  is the band-gap energy, The presence of a single slope in the curves in the plot of  $(\alpha h\nu)^2$  versus  $h\nu$  of CFTSe suggests that the film is in nature with direct allowed transition.  $r$  value representing the optical transmission mode; when  $r = 1/2$  the transition mode is direct allowed,  $r = 3/2$  is direct forbidden,  $r = 2$  is indirect allowed, and  $r = 3$  is indirect forbidden.

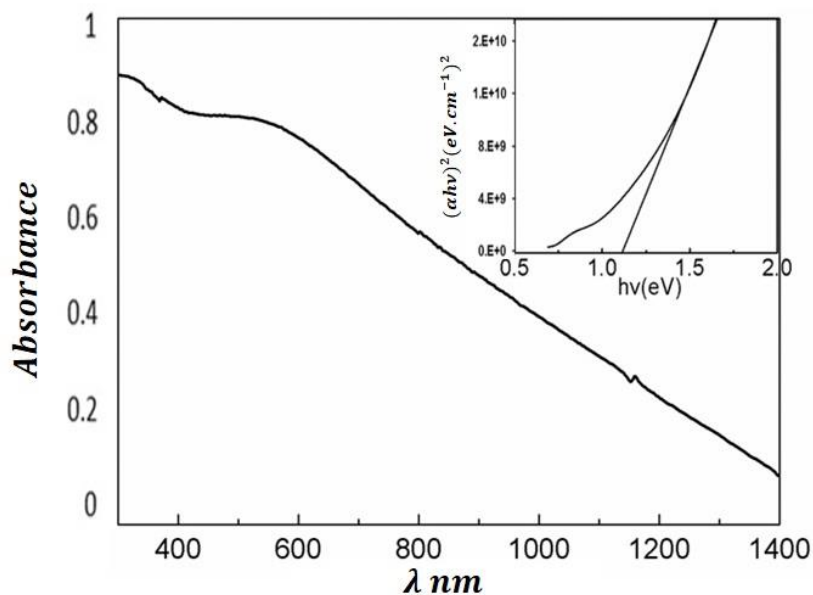


**Figure 4-** Absorption spectra and band-gap of CFTSe nanofilms.

Under chopped light illumination condition, PEC responses of FTO/CFTSe thin films were studied.

Figure- 5a shows that the I-V curves were decreased from -0.4 to 0 V, which represents the cathodic potential scan range, indicating p-type CFTSe thin films. The deposition of Pt thin films onto the surface of CFTSe films can enhance their catalysis characteristics [15]. The deposition of n-type CdS thin films to form a p-n junction with CFTSe can also separate the photo-generated charge carriers efficiently [16]. All of these results are confirmed by the current-potential curves which are shown in Figure- 5a. The I-t curves in Figure- 5b, show that the photocurrent densities of FTO/CFTSe are about  $9 \mu\text{A}/\text{cm}^2$ . After depositing of CdS and Pt thin films, the fabrication of FTO/CFTSe/CdS/Pt can enhance the photo-electrochemical properties of FTO/CFTSe greatly, due to the fact that the photocurrent density of FTO/CFTSe/Pt and FTO/CFTSe/CdS/ Pt thin films were increased to 15 and  $38 \mu\text{A}/\text{cm}^2$ , respectively

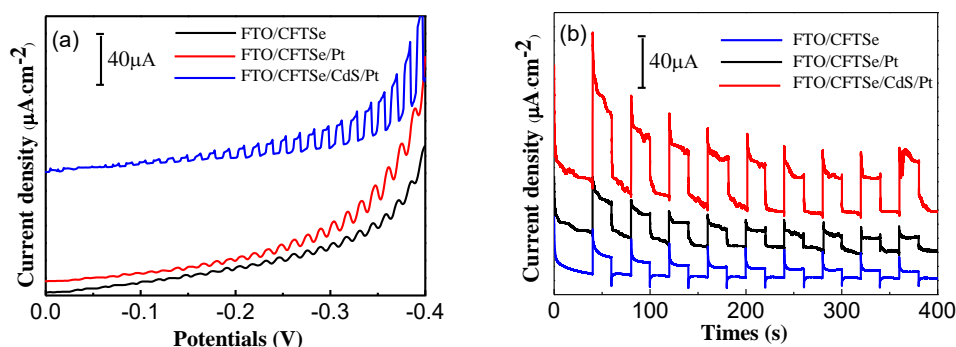


**Figure 5-** I-V (a) and I-t (b) curves of FTO/CFTSe, FTO/CFTSe/Pt and FTO/CFTSe /CdS/Pt.

## Conclusions

In conclusion, CFTSe nanoparticles were prepared by a convenient hot-injection method. The as-synthesized CFTSe nanoparticles were well dispersed and the averaged particles sizes were about 10 nm. From the optical absorption spectra, the energy band gap of CFTSe nanofilms was estimated to be about 1.16 eV. The fabrication of FTO/CFTSe/CdS/Pt enhanced the photo-electrochemical properties of FTO/CFTSe greatly, which confers a contribution to the development of CFTSe nanoparticles and their potential application in photovoltaic applications.

## References

1. Yike Liu, Mengmeng Hao, Jia Yang, Liangxing Jiang, Chang Yan, Chun Huang, Ding Tang, Fangyang Liu and Yexiang Liu. **2014**. Colloidal synthesis of  $\text{Cu}_2\text{FeSnSe}_4$  nanocrystals for solar energy conversion, *Materials Letters*, **136**: 36-309, <https://doi.org/10.1016/j.matlet.2014.08.072>
2. Jicheng Zhou, Zhibin Ye, Yunyun Wang, Qiang Yi and Jiawei Wen. **2015**. Solar cell material  $\text{Cu}_2\text{FeSnS}_4$  nanoparticles synthesized via a facile liquid reflux method, *Materials Letters*, **140**: 119-122, <https://doi.org/10.1016/j.matlet.2014.11.004>
3. X.Fontané, V.Izquierdo-Roca, E.Saucedo, S.Schorr, V.O.Yukhymchuk, M.Ya.Valakh, A.Pérez-Rodríguez and J.R.Morante. **2012**. Vibrational properties of stannite and kesterite type compounds: Raman scattering analysis of  $\text{Cu}_2(\text{Fe,Zn})\text{SnS}_4$ ” *Journal of Alloys and Compounds*, **539**: 190-194, <https://doi.org/10.1016/j.jallcom.2012.06.042>
4. Xin Jiang, Wei Xu, Ruiqin Tan, Weijie Song and Jianmin Chen. **2013**. Solvothermal synthesis of highly crystallized quaternary chalcogenide  $\text{Cu}_2\text{FeSnS}_4$  particles, *Materials Letters*, **102–103**: 39-42, <https://doi.org/10.1016/j.matlet.2013.03.102>
5. C. Rincón, M. Quintero, E. Moreno, Ch. Power, E. Quintero, J.A. Henao, M.A. Macías, G.E. Delgado, R. Tovar and M. Morocoima. **2011**. X-ray diffraction, Raman spectrum and magnetic susceptibility of the magnetic semiconductor  $\text{Cu}_2\text{FeSnS}_4$ , *Solid State Communications*, **151**(13): 947-951, <https://doi.org/10.1016/j.ssc.2011.04.002>
6. M. Adelifard. **2016**. Preparation and characterization of  $\text{Cu}_2\text{FeSnS}_4$  quaternary semiconductor thin films via the spray pyrolysis technique for photovoltaic applications, *Journal of Analytical and Applied Pyrolysis*, **122**: 209-215, <https://doi.org/10.1016/j.jaap.2016.09.022>
7. Tulay Aygan Atesin, Sajid Bashir and Jingbo Louise Liu. **2019**. Nanostructured Materials for Next-Generation Energy Storage and Conversion: Photovoltaic and solar Energy, Springer,



- <https://doi.org/10.107/978-3-662-59594-7>
8. Liang Shi and Quan Li. **2011**. Thickness tunable  $\text{Cu}_2\text{ZnSnSe}_4$  nanosheets, *CrystEngComm*, **13**(21): 6507-6510, DOI: [10.1039/C1CE05746D](https://doi.org/10.1039/C1CE05746D)
  9. Ubaidah Syafiq, Narges Ataollahi, Rosa Di Maggio, and Paolo Scardi. **2019**. Solution-Based Synthesis and Characterization of  $\text{Cu}_2\text{ZnSnS}_4$  (CZTS) Thin Films, *Molecules*. **24**(19): 3454, doi: [10.3390/molecules24193454](https://doi.org/10.3390/molecules24193454)
  10. Donglin XIA, Yuchen ZHENG, Pan LEI and Xiujian ZHAO. **2013**. Characterization of  $\text{Cu}_2\text{ZnSnS}_4$  thin films prepared by solution-based deposition techniques, *Physics Procedia*, **48**: 228 – 234, DOI: [10.1016/j.phpro.2013.07.036](https://doi.org/10.1016/j.phpro.2013.07.036)
  11. H. Yoo, R.A. Wibowo, A. Hölzing, R. Lechner, J. Palm, S. Jost, M. Gowtham, F. Sorin, B. Louis and R. Hock. **2013**. Investigation of the solid state reactions by time-resolved X-ray diffraction while crystallizing kesterite  $\text{Cu}_2\text{ZnSnSe}_4$  thin films, *Thin Solid Films*, **535**: 73–77, <http://dx.doi.org/10.1016/j.tsf.2013.01.054>
  12. I.V. Dudchak and L.V. Piskach. **2003**. Phase equilibria in the  $\text{Cu}_2\text{SnSe}_3$ – $\text{SnSe}_2$ – $\text{ZnSe}$  system”, *Journal of Alloys and Compounds*, **351**(1–2): 145-150, [https://doi.org/10.1016/S0925-8388\(02\)01024-1](https://doi.org/10.1016/S0925-8388(02)01024-1)
  13. B. M. Caruta. **2006**. *Focus on Nanomaterials Research*, Nova science publisher Inc. New York,
  14. Mohammed. A. Hameed, Omar Abdulsada Ali, Sarmed S.M. Al-Awadi. 2020. Optical properties of Ag-doped nickel oxide thin films prepared by pulsed-laser deposition technique, *Optik - International Journal for Light and Electron Optics*, 206, 164352. DOI: [10.1016/j.ijleo.2020.164352](https://doi.org/10.1016/j.ijleo.2020.164352)
  15. Shuo Wang , Rui-xin Ma , Cheng-yan Wang , Shi-na Li and Hua Wang. **2017**. Effects of K ions doping on the structure, morphology and optical properties of  $\text{Cu}_2\text{FeSnS}_4$  thin films prepared by blade-coating process, *Optoelectronics Letters*, **13**(4): 291-294, DOI: [10.1007/s11801-017-7108-4](https://doi.org/10.1007/s11801-017-7108-4)
  16. Alessia Le Donne, Vanira Trifiletti and Simona Binetti. **2019**. New Earth-Abundant Thin Film Solar Cells Based on Chalcogenides, *Frontiers in Chemistry, Physical Chemistry and Chemical Physics*, **7**: 1-13, <https://doi.org/10.3389/fchem.2019.00297>